ELSEVIER

PII: S0032-3861(97)00044-X

Polymer Vol. 38 No. 20, pp. 5073–5078, 1997
© 1997 Elsevier Science Ltd
Printed in Great Britain. All rights reserved
0032-3861/97/$17.00 + 0.00

Forward recoil spectrometry study of the diffusion of PMDA/ODA-based poly(amic ethyl esters)

Nancy C. Stoffel*, Sweta Chandra and Edward J. Kramer
Department of Materials Science and Engineering, Bard Hall, Cornell University, Ithaca, NY 14853, USA

and Willi Volksen and Thomas P. Russell
IBM Almaden Research Center, 650 Harry Rd, San Jose, CA 95120, USA
(Received 5 September 1996; revised 2 January 1997)

The poly(amic ethyl esters) (PAEs) of pyromellitic dianhydride/4,4′-oxydianiline (PMDA/ODA) were prepared in three isomeric forms, with *meta*-linkages, *para*-linkages and randomly alternating *meta*- and *para*-linkages (referred to as mixed PAEs). In addition to the normal PAEs (which contained only hydrogen and which were cast as base layers for diffusion studies), each of these isomeric PAE was synthesized in two other forms: (1) labelled with deuterium on the ODA segments, and (2) labelled with deuterium on the ethyl ester moiety to allow determination of the imide fraction, **f**. Forward recoil spectrometry (FRES) was utilized to provide information about the polyimide–polyimide interface by measuring the depth profile of hydrogen and deuterium for bilayer samples consisting of a thick non-deuterated base layer, and a thin deuterated tracer layer. FRES measurements indicated that the interdiffusion distance, w, decreased markedly with increasing imidization temperature, T_i. For base layers prepared from *N*-methylpyrrolidone, w for the *para*- and mixed PAE base layers decreased more rapidly with T_i than with w for the *meta*-PAE base layers. However, these differences were found to result from the differences in imidization kinetics of the various isomers with **f** increasing more rapidly with T_i for *para*- and mixed PAE than for the *meta*-PAE. Nevertheless, when w was plotted as a function of **f**, all of the isomers exhibited similar behaviour, i.e. w decreased steadily as the imide fraction **f** approached 1. Base layers cast from dimethyl sulfoxide did not show differences in either **f** or w after imidization at a given T_i. © 1997 Elsevier Science Ltd.

(Keywords: polyimide; interdiffusion; forward recoil spectrometry)

INTRODUCTION

Polyimides are important materials in the electronics industry due to their superior thermal and mechanical properties. They are often used as an interlayer dielectric material, replacing inorganics such as silicon dioxide or alumina, because of their relatively low dielectric constant. However, polyimide layers, sequentially deposited, display poor self-adhesion, hence, raising processing issues and reliability concerns for multi-level polyimide structures. The poor self-adhesion is due in part to the method of preparation of polyimide layers. Generally, they are first prepared as a polyimide precursor linked by amide bonds, such as a poly(amic acid) (PAA) or a poly(amic alkyl ester). These precursors are soluble in organic polar solvents such as *N*-methylpyrrolidone (NMP), and a layer is spun cast from solution. This layer is dried, and then thermally treated, to form the final polyimide structure via a ring-closing reaction. If this base layer is fully converted into polyimide, subsequent layers spun-cast upon this first fully imidized layer will adhere only poorly to it because the polyimide and the polyimide precursor are essentially immiscible. Hence, the practice of initially treating the base layer at a 'soft-bake' temperature has arisen[1]. In this case, the underlying layer is not fully converted into polyimide, but retains a fraction of its initial acid or alkyl ester moieties. The fraction of the initial acid or alkyl ester moieties converted into imide is referred to as the imide fraction or degree of imidization, **f**. In some cases, it is not possible to work with a partially cured layer and other methods are used to improve the adhesion of the two polyimide layers, including plasma treatments and adhesion promoters.

The adhesive strength of the polyimide–polyimide interface has been correlated with the amount of intermixing across the interface[2,3]. Brown *et al.*[2] demonstrated that for the polyimide pyromellitic dianhydride/4,4′-oxydianiline (PMDA/ODA) produced by thermally converting spun-cast PAA into the polyimide, the distance of interdiffusion, w, depended upon the imidization temperature, T_i, of the base layer. The corresponding interfacial fracture energy, G_c, decreased rapidly as T_i was increased from 150 to 200°C. Tead *et al.*[4,5] verified the relationship between T_i and w for PAA precursors and also found that, in the absence of solvents, thermally activated diffusion does not occur for the PMDA/ODA polyimide system.

* To whom correspondence should be addressed

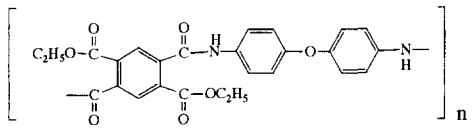

para-PAE

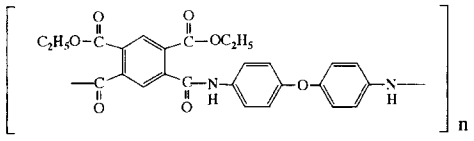

meta-PAE

Figure 1 Schematic representation of the chemical repeat units for the *para*- and *meta*-PAE isomers based on PMDA/ODA. The mixed isomer is a random mixture of the *para* and *meta* connections along the main chain

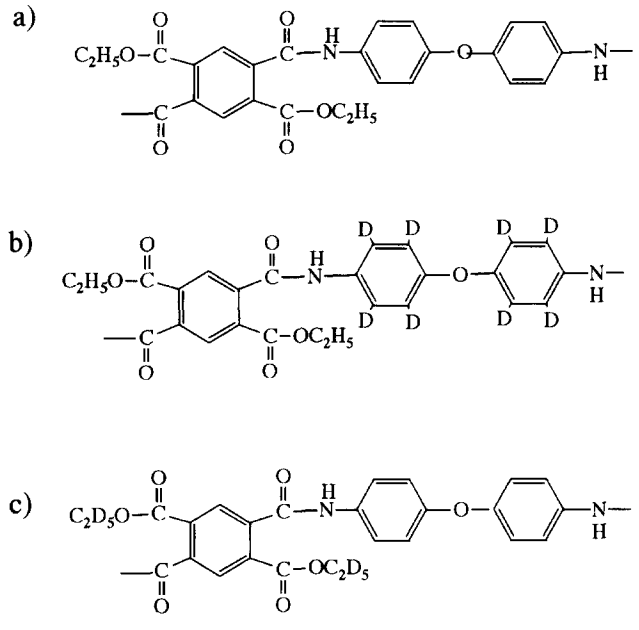

Figure 2 (a) PAE: non-deuterated version, used as base layer; (b) dPAE: partially deuterated in backbone, used as diffusion tracer; (c) PAdE: deuterated in the ester moiety used as an imidization indicator

Here, we investigate in more detail the factors controlling the amount of intermixing across the polymer–polymer interface, with the intention of using this knowledge to improve the processing of polyimides. We explore the role played by molecular architecture, imide fraction and spin-casting solvent in the construction of the interface. Forward recoil spectrometry (FRES) is utilized to provide information about the polyimide–polyimide interface by measuring the depth profile of hydrogen and deuterium for bilayer films consisting of one non-deuterated and one deuterated layer.

We have utilized the poly(amic ethyl ester) (PAE) precursor of the polyimide of PMDA/ODA. These precursors are superior to PAA precursors due to their greater hydrolytic stability and stable solution viscosity as well as the fact that they imidize in a temperature regime that is both higher and more extended than that of PAA[6,7]. Additionally, the alkyl ester precursors may be prepared in three structural isomeric forms, with all *meta*-linkages, or with all *para*-linkages, or with a main chain consisting of randomly alternating *meta*- and *para*-linkages (referred to, respectively, as *m*-, *p*- and mixed isomers) as shown in *Figure 1*. The *para*-precursor exhibits solution viscosities substantially higher than those of the *meta*-precursor and has a larger persistence length of 4.5 nm compared to 1.8 nm for the *meta*-isomer[8].

For our experiments, a polymer in each of the isomeric forms was also prepared in three different ways (making a total of nine different polymers) in order to provide information about interdiffusion and degree of conversion into the polyimide form. The three classes are shown in *Figure 2* for the *para*-isomer. *Figure 2a* shows the non-deuterated PAE. The molecule shown in *Figure 2b* is deuterated on the ODA segment in order to be useful as a tracer molecule in diffusion studies and is referred to as dPAE. *Figure 2c* shows the third type of polymer synthesized with deutrium substituted on the ethyl ester moiety and is referred to as PAdE. This version allows us to determine the degree of conversion of the precursor polymer into polyimide using FRES. FRES analysis has an advantage over other methods used to determine imidization in that it provides information about the imide fraction as a function of depth[9].

We chose to prepare solutions of these polymers in both NMP and dimethyl sulfoxide (DMSO), because of experimental data[9] showing profound differences in the rate and depth dependence of imidization for samples prepared from these two solvents.

EXPERIMENTAL

Materials' preparation

The preparation of PAE materials was similar in all cases. The only differences were the use of perdeuterated ODA in the case of dPAE and perdeuterated ethanol to synthesize the monomer utilized in the preparation of PAdE. A complete description of the polymerization is published elsewhere[6,7,9] and is outlined below and illustrated in *Figure 3*.

PMDA was first converted into diethyl dihydrogen pyromellitate by suspending the PMDA in dichloromethane and adding ethanol and dry triethylamine in the molar ratio 5/1 for each unit of PMDA. The mixture was stirred for 16 h to ensure completion of the amine addition, then the dichloromethane was evaporated under vacuum, and the amorphous residue diluted with distilled water. Subsequent conversion of the diethyl ammonium salt into the neutral allowed extraction of the more soluble *meta*-isomer from the isomer mixture with ethyl acetate. Recrystallization of the *meta*- and *para*-isomers from butyl acetate yielded monomers with greater than 99% isomeric purity.

The diester diacid was then activated to enable the monomer to enter a polymer forming reaction by conversion into diethylpyromellitate diacyl chloride. The diacid was suspended in ethyl acetate, and an excess of oxalyl chloride was added slowly over a period of 8 h. Evaporation of the solvent yielded a crystalline residue which was recrystallized from boiling hexane for the *meta*-isomer and from cyclohexane for the *para*-isomer.

The final step in the synthesis involved reacting the diethylpyromellitate diacyl chloride with ODA in the presence of pyridine, an acid scavenger, to form

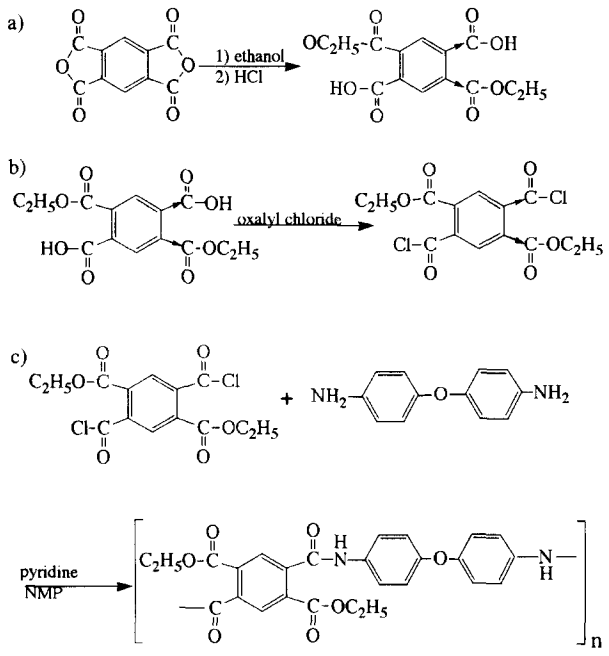

Figure 3 (a) Preparation of diethyl dihydrogen pyromellitate; the diethyl diacid isomers may be separated by selective solubility at this point. (b) Activation of the monomer by conversion into diethyl pyromellitate diacyl chloride. (c) Polymerization to prepare the PAE

Table 1 Intrinsic viscosity and molecular weights of the *para*-PAE and *meta*-PAE precursors of PMDA/ODA

	$[\eta]$	M_w
para-PAE	140	41 000
meta-PAE	55	37 000

the PAEs. This was accomplished by dissolving the freshly sublimed ODA and pyridine in NMP, which had been distilled out of P_2O_5 and a slight excess of pyridine based on diacyl dichloride. The diacyl dichloride, dissolved in tetrahydrofuran, was slowly added to the reaction vessel, and the reaction mixture was stirred under nitrogen for 3 h. The polymerization mixture was then precipitated into distilled water in a Waring blender. The precipitate was filtered and washed with distilled water, followed by ethanol and then ethyl acetate. Finally, the powder was dried in a vacuum oven at 50°C for 24 h. Varying the deuterium labelling on the polymer was accomplished by using appropriately deuterium labelled initial reactants.

Experimental molecular weight values were determined through the solution properties. Measurements of dilute solution viscosities were made using a Cannon 75 Ubelohde viscometer maintained at 27.5°C with an automatic timer. Dilute solutions were prepared of the non-deuterated PAE isomers in NMP and filtered through a 1 μm filter. Elution times for solvent and solutions were all above 150 s. Measurements were made at four different concentrations in a concentration regime which yielded relative viscosities of less than 2. The reduced and inherent viscosities were calculated, and found to be linear. The intrinsic viscosity, $[\eta]$, was found by extrapolating to zero concentration, in accord with the Huggins and Kraemer relations:

$$\left(\frac{\eta_{sp}}{c}\right) = [\eta] + k'[\eta]^2 c + \cdots$$

$$\ln\left(\frac{\eta_{rel}}{c}\right) = [\eta] + (k' - 1/2)[\eta]^2 c + \cdots$$

Weight average molecular weights, M_w, were then calculated from the correlation between intrinsic viscosity and M_w (determined by light scattering), established by Cotts and Volksen[8], for the unlabelled *meta*- and *para*-isomers of the PAE precursors of PMDA/ODA. Consistent with these results, we found the intrinsic viscosity values to be greater for the *para*-isomers than for the *meta*-isomers. The experimentally determined intrinsic viscosities $[\eta]$ and the corresponding molecular weights M_w are shown in *Table 1*.

Sample preparation and analysis

Samples designed for measuring interdiffusion were prepared for each of the non-deuterated precursor polymers (*m*-PAE, *p*-PAE and mixed PAE) and for each of the deuterated tracer polymers (*m*-dPAE, *p*-dPAE and mixed dPAE) using both NMP and DMSO as casting solvents. These diffusion samples were analysed using FRES. The samples consisted of a base layer of non-deuterated PAE, thermally treated to undergo partial imidization and a thin dPAE tracer layer spun-cast on to the base layer. The geometry chosen was that of a thin layer of tracer diffusing into a semi-infinite base layer. The samples prepared for FRES analysis were made by preparing a base layer of approximately 2 μm thickness spun-cast from an 8–10 wt% solution of the non-deuterated polymer at 600 rev min^{-1} for 60 s on to 3 in ($\simeq$ 7.6 cm) diameter chromium-coated silicon wafers. These wafers were then dried at 80°C for 1 h in a vacuum oven, diced into pieces approximately 15 mm square and heated to undergo partial to full imidization. Heat treatments below 280°C were performed for 1 h in a preheated vacuum oven, while heat treatments above 280°C were carried out in a quartz tube furnace under flowing argon. These treatments required a 15°C min^{-1} ramp to the desired temperature, where the sample was held for 1 h, after which it was cooled at 5°C min^{-1}. A thin tracer dPAE layer of approximately 600 Å thickness was spun on to the thermally treated base layer. The bilayer samples were then dried at 80°C to remove excess of solvent.

Forward recoil spectrometry was used to determine the concentration profile of the deuterated PAE species with the partially imidized base layer. The experimental profiles of the volume fraction of dPAE, ϕ_{dPAE}, were analysed using the solution of Fick's second law of diffusion for a sample consisting of a thin layer of thickness h on a semi-infinite non-deuterated polymer film, viz.[10]

$$\phi_{dPAE}(x) = \frac{1}{2}\left\{\operatorname{erf}\frac{h+x}{w} + \operatorname{erf}\frac{(h-x)}{w}\right\} \qquad (1)$$

where w = interdiffusion distance $[(4Dt)^{0.5}]$, t = diffusion time, and D = diffusion coefficient.

Since D in the solvent swollen base layer is almost surely both time and concentration dependent, w should be interpreted strictly as an interpenetration distance or a distance over which intermixing occurs at the interface. The theoretical profile was convoluted with a Gaussian function representing the instrumental resolution and then compared to the experimental profile. The thickness of the tracer layer, h, was determined by integrating ϕ_{dPAE} and w was varied to optimize the fit. *Figure 4* shows a typical FRES spectrum, fit using equation (1).

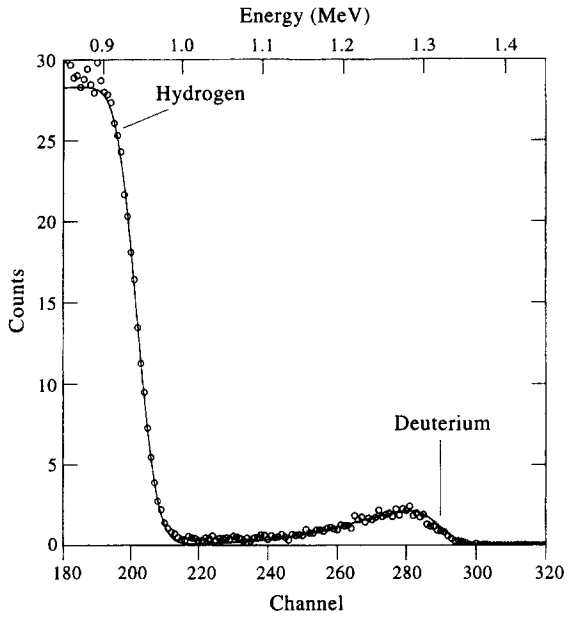

Figure 4 Typical FRES spectra fora bilayer diffusion sample is shown. The solid line corresponds to a simulation using the solution to Fick's second law, convoluted with a Gaussian resolution function. The best fit corresponds to a *w* of 167 nm

The imide fraction, **f**, of a PAdE sample was also determined using FRES where the PAdE sample was processed in an identical manner to the base layer diffusion sample. The imidization of samples prepared from NMP differed, depending on the isomer. In addition, the imidization behaviour of the mixed and *para*-isomers prepared from NMP was depth dependent, with the region within 2000 Å of the surface showing a smaller **f** than the bulk. Samples prepared from DMSO as solvent did not display either isomer-dependent or depth-dependent imidization behaviour. A full report of the imidization behaviour of these structural isomers is reported elsewhere[9,11]. The differences in imidization behaviour of samples cast from different solvents prompted us to include a comparison of samples cast from different solvents in this diffusion study.

RESULTS AND DISCUSSION

Figure 5 is a plot of interdiffusion distance *w versus* imidization temperature for the *m*-, *p*- and mixed PAE base layers and the PAA base layer, using the mixed dPAE tracer layer (prepared from NMP solvent). The interdiffusion distance decreases sharply as the imidization temperature of the base layer increases. Consequently, the interdiffusion appears to be influenced by both the leaving group and the isomeric identity of the base layer. However, a more unified picture emerges if one considers the dependence of interdiffusion distance on the imide fraction, **f**, of the base layers. Shown in *Figure 6* is *w* of the dPAE tracer polymer as a function of **f**, with a base layer formed by spin-casting the various isomers from NMP. To within experimental error, the data collapse to a single curve, which demonstrates that the controlling factor in determining *w* is the imide fraction of the base layer and that the isomeric identity of the base layer contributes only in that it can affect **f** for a given annealing treatment.

Measurement of interdiffusion distance in samples where the base layer imide fraction **f** was below 0.3 was

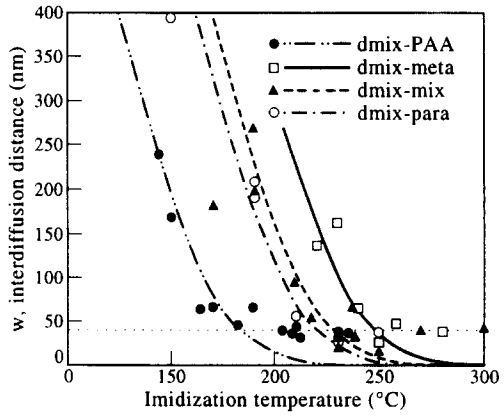

Figure 5 Interdiffusion distance is plotted against the imidization temperature of the base layer for *m*-, *p*- and mixed PAE samples prepared from NMP solvent. Mixed dPAE tracer was used for all of the bilayer samples. The horizontal dotted line represents the minimum detectable diffusion distance

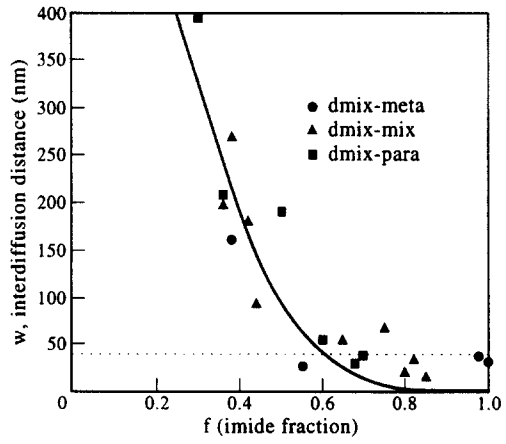

Figure 6 Interdiffusion distance is plotted against the imide fraction of the base layer for *m*-, *p*- and mixed PAE samples prepared from NMP. Mixed dPAE tracer was used for all of the bilayer samples. The dotted line represents the minimum detectable diffusion distance

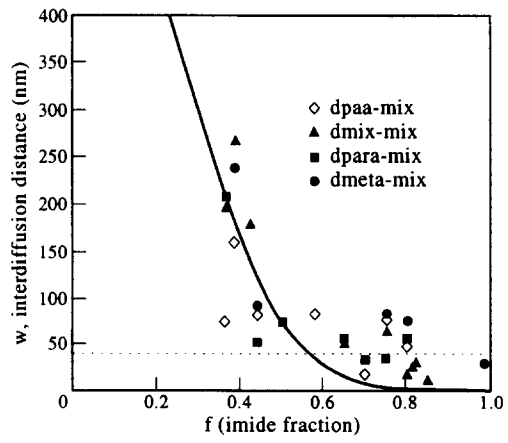

Figure 7 Interdiffusion distance, measured in bilayer samples prepared from NMP, is plotted against imide fraction of the mixed PAE base layer. *Meta*-, *para*- and mixed dPAE are all utilized as tracer layers. The dotted line represents the minimum detectable diffusion distance

subject to large errors, making quantitative comparison difficult. It should be noted that, in some cases, the solvent appeared to dissolve the base layer so that a portion of this layer was washed away in the spin-casting process. Interdiffusion distances measured for base layers with $\mathbf{f} > 0.7$ are of the same order of magnitude as the resolution of FRES (600 Å) and for this reason do not give an accurate indication of the width of the interface. The interdiffusion distance may continue to decrease with **f** to values below 60 nm for $\mathbf{f} > 0.7$, but these values would not be measurable by FRES.

The strong dependence of w on **f** of the base layer probably occurs because the base 'polyimide' layer and the tracer dPAE layer become less miscible as **f** of the base layer increases. An increase in **f** of the base layer means that an increasing fraction of the amide linkages are being converted into imide rings. Consequently, the polymers in the base and tracer diffusion layers are becoming increasingly dissimilar with increasing **f**. As is well known, miscibility between two different polymers is the exception to the rule, since small non-favourable interactions are sufficient to overcome any small entropic gain upon mixing. Thus, the larger the **f** the more dissimilar the polymers in the base and tracer diffusion layers become. This dissimilarity, in turn, would result in a decrease in the interfacial width[12].

The effect of using different dPAE isomers as tracers is shown in *Figure 7*. In this diagram, w is plotted *versus* **f** for a base layer produced from one PAE isomer (mixed PAE prepared from NMP solvent). No consistent difference in w is observed for the different dPAE isomers as tracers. Also, using a dPAA tracer did not seem to alter the amount of interdiffusion. Similar results were obtained for base layers of the other isomers of PAE.

Results for bilayer diffusion samples prepared from DMSO differed from those prepared from NMP in that they did not show any difference in w *versus* T_i for base layers produced from the different PAE isomers. Rather, as shown in *Figure 8*, the data for the *m*-, *p*- and mixed PAE base layers all appear to fall on the same curve. The difference in the interdiffusion behaviour seen for the different solvents corresponds to a difference in imidization kinetics for samples prepared from NMP and DMSO. This fact is demonstrated by the data in *Figures 9a* and *9b* where the imide fraction of a bulk

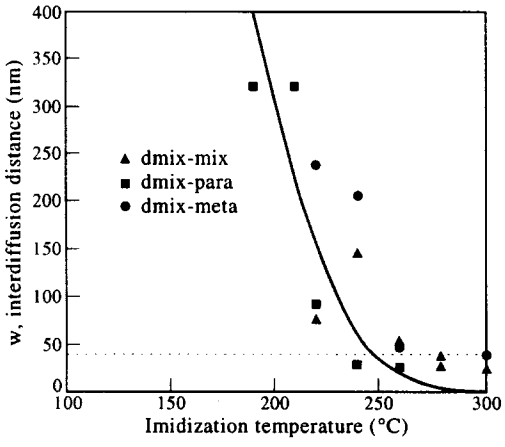

Figure 8 Interdiffusion distance of an isomeric dPAE layer into its isomeric base pair is shown as a function of base layer imidization temperature T_i for samples cast from DMSO. The dotted line represents the minimum detectable diffusion distance

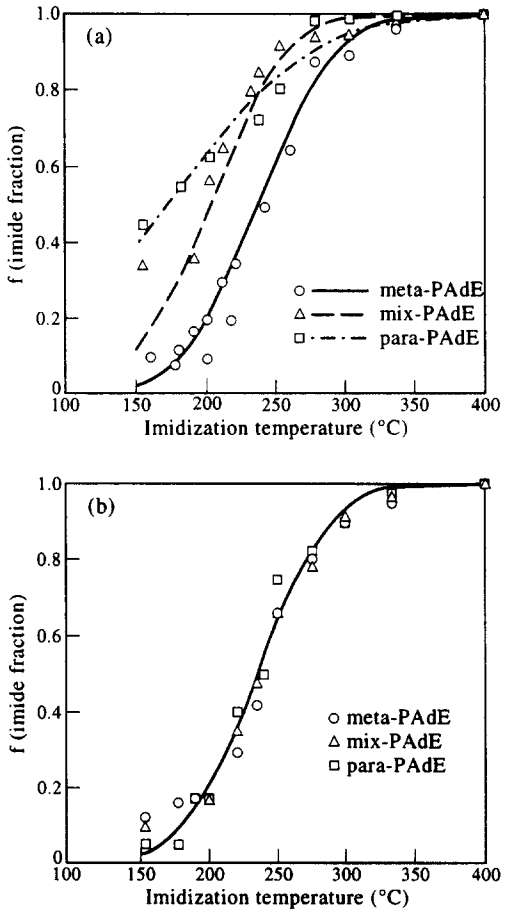

Figure 9 FRES was used to determine imide fraction in *m*-, *p*- and mixed PAdE samples annealed for 1 h at T_i: (a) results for samples cast from NMP; (b) results for samples cast from DMSO

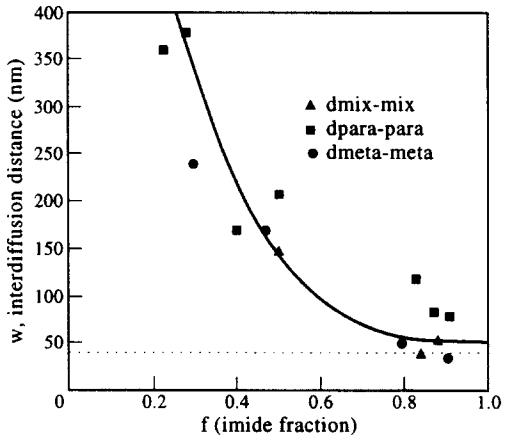

Figure 10 Interdiffusion distance of bilayer samples prepared from DMSO is plotted for isomeric base–tracer pairs as a function of base layer imide fraction

sample is plotted as a function of T_i for films cast from NMP and DMSO, respectively. It is seen that the mixed and *p*-PAdE samples prepared from NMP have a higher imide fraction than have similar samples prepared from DMSO. In contrast, the *m*-PAdE samples display similar behaviour when spun-cast from both solvents. The differences in imidization kinetics for the NMP- and DMSO-cast samples arise from differences in solvent retention for the two systems[9]. In *Figure 10*, w is shown as a function of **f** for the samples cast from DMSO. The data fall on a curve similar to the one for the samples cast

from NMP. The differences in interdiffusion distance observed after a given heat treatment for samples prepared from NMP and DMSO can thus be attributed primarily to differences in imidization behaviour of the base layer.

While FRES was effective for investigating the relationship between w and T_i or **f** it is limited by its rather poor depth resolution of 800 Å. The instrumental resolution limitations are due primarily to statistical straggling of the hydrogen and deuterium nuclei in the Mylar foil in front of the detector. Higher resolution depth profiling techniques, such as dynamic secondary ion mass spectrometry, time-of-flight FRES, nuclear reaction analysis and neutron reflectivity are currently being used to investigate sharper interfaces. This regime corresponding to high imide fractions and high T_i is of great importance since we know that the interface fracture toughness G_c continues to decrease with increasing imidization temperature T_i, even for temperatures where the differences in w are not discernible using FRES.

CONCLUSIONS

Using FRES, we have investigated the relationship between imidization temperature, imide fraction and interdiffusion distance for PMDA/ODA polyimide derived from isomeric PAEs. The interdiffusion distance w is mainly a function of **f**, decreasing steadily as the imide fraction **f** is increased towards 1. The solvent and isomeric character of the base layer contribute to changes in the interdiffusion distance only as much as they affect **f**. For base layer samples cast from NMP, large differences could be discerned in w for a given T_i. However, these differences can be attributed to the values of **f**, which are quite different for the *meta*-isomer as compared to the *para*- and mixed isomers. Samples cast from DMSO did not show differences in either **f** or w after imidization at a given T_i. In addition, the value of w exhibited only a weak dependence on the isomeric nature of the tracer layer cast from both NMP and DMSO.

ACKNOWLEDGEMENTS

We gratefully acknowledge the primary financial support of the SRC Corporation, through the Electronic Packaging Program. Additional support was received from IBM and the Cornell Electronic Packaging Alliance. We benefited from the use of the facilities of the Cornell Materials Science Center, which is funded by the DMR–MRL program of the NSF.

REFERENCES

1. Czornyj, G., Chen, K. R., Prada-Silva, G., Arnold, A., Souleotis, H., Kim, S., Ree, M., Volksen, W., Dawson, D. and DiPietro, R., in *Proceedings of the 42nd Electronic Components Technology Conference*, 1992, p. 682.
2. Brown, H. R., Yang, A. C. M., Russell, T. P., Volksen, W. and Kramer, E. J., *Polymer*, 1988, **29**, 1807.
3. Stoffel, N. C., Kramer, E. J., Volksen, W. and Russell, T. P., *Mat. Res. Soc. Sym. Proc.*, Pittsburgh, USA, 1993, **305**, 153.
4. Tead, S. F., Kramer, E. J., Russell, T. P. and Volksen, W., *Mat. Res. Soc. Sym. Proc.*, **153**, 239.
5. Tead, S. F., Kramer, E. J., Russell, T. P. and Volksen, W., *Polymer*, 1992, **16**, 3382.
6. Volksen, W., Yoon, D. Y., Hedrick, J. L. and Hofer, D., in *MRS Symposia Proceedings*, Vol. 227. Anaheim, CA, April 1991, p. 23.
7. Volksen, W., *Interdisciplinary Symposium*, Division of Polymer Chemistry, American Chemical Society, San Diego, CA, 22–25 Jan., 1990, C-1.
8. Cotts, P. M. and Volksen, W., *Polymer News*, 1990, **15**, 106.
9. Stoffel, N. C., Kramer, E. J., Volksen, W. and Russell, T. P., *Polymer*, 1993, **34**, 4524.
10. Crank, J., *The Mathematics of Diffusion*, 2nd edn. Oxford University Press, Oxford, UK, 1985, p. 15.
11. Tead, S. F., Kramer, E. J., Russell, T. P. and Volksen, W., *Polymer*, 1990, **31**, 520.
12. Flory, P. J., *Principles of Polymer Chemistry*. Cornell University Press, Ithaca, NY, 1953, p. 301.